

## LiCoO<sub>2</sub>-Supported Catalysts for Hydrogen Generation from Sodium Borohydride Solution

O. V. KOMOVA<sup>1</sup>, V. I. SIMAGINA<sup>1</sup>, N. V. KOSOVA<sup>2</sup>, O. V. NETSKINA<sup>1</sup>, G. V. ODEGOVA<sup>1</sup>, T. YU. SAMOILENKO<sup>1</sup>, E. T. DEYYATKINA<sup>2</sup> and A. V. ISHCENKO<sup>1</sup>

<sup>1</sup>*Boriskov Institute of Catalysis, Siberian Branch of the Russian Academy of Sciences, Pr. Akademika Lavrentieva 5, Novosibirsk 630090 (Russia)*

*E-mail: komova@catalysis.nsc.ru*

<sup>2</sup>*Institute of Solid State Chemistry and Mechanochemistry, Siberian Branch of the Russian Academy of Sciences, Ul. Kutateladze 18, Novosibirsk 630128 (Russia)*

### Abstract

Effect of LiCoO<sub>2</sub> support prepared by traditional ceramic and mechanochemical route on the activity of Rh and Pt catalysts in the reaction of NaBH<sub>4</sub> hydrolysis was studied and compared with traditional supports, such as  $\gamma$ -Al<sub>2</sub>O<sub>3</sub>, TiO<sub>2</sub> (anatase) and carbon (sibunit). Catalysts supported on LiCoO<sub>2</sub> prepared using mechanical activation were found to have the highest catalytic activity. However, the endurance tests of 1 % Rh–LiCoO<sub>2</sub> и 1 % Pt–LiCoO<sub>2</sub> catalysts showed their gradual degradation. To understand the reason of this phenomenon, the interaction of LiCoO<sub>2</sub> with NaBH<sub>4</sub> solution was studied by XRD, FTIR, DRS and TEM.

### INTRODUCTION

The development of fuel cells and their wide application are impossible without developing highly efficient and safe technologies for obtaining pure hydrogen and its storage. According to many researchers [1–4], catalytic hydrolysis of NaBH<sub>4</sub> is a promising method for hydrogen synthesis for use in portable fuel cells.

Different catalytic systems have been suggested for the NaBH<sub>4</sub> hydrolysis reaction. In recent publications, one can find information on the use of ruthenium catalysts supported on anion-exchange resins (A-26, IRA-400) [2, 5, 6], platinum group metals on various supports [3, 4, 7], cobalt borides [8, 9], nickel boride [10] and finely dispersed metallic nickel and cobalt [11, 12] in this reaction. In the last few years, several publications on the use of catalysts containing platinum group metals supported on LiCoO<sub>2</sub> appeared in the literature [3, 13–15]. LiCoO<sub>2</sub> is well known cathode material for lithium ion batteries, widely produced by different companies. However, the authors used

commercially produced LiCoO<sub>2</sub> missing the description of preparation method and of characteristics of as-used LiCoO<sub>2</sub>. In addition, there is no information on the stability of this catalytic system under endurance tests.

In the present paper, LiCoO<sub>2</sub> supports were prepared by two methods: traditional ceramic and using preliminary mechanical activation (MA) of reagent mixture. Their effect on the activity of Pt and Rh catalysts in the NaBH<sub>4</sub> hydrolysis was studied and compared with traditional supports, such as  $\gamma$ -Al<sub>2</sub>O<sub>3</sub>, TiO<sub>2</sub> (anatase) and carbon (sibunit). The stability of LiCoO<sub>2</sub> in the NaBH<sub>4</sub> solution was also investigated.

### EXPERIMENTAL

#### *Catalyst preparation*

Aqueous solutions of RhCl<sub>3</sub> (Aurat) and H<sub>2</sub>PtCl<sub>6</sub> (Aurat) were used for the catalyst preparation. Water was added to the weighted support sample and stirred for 5 min using a mag-

TABLE 1  
Specific surface area of LiCoO<sub>2</sub> samples

Sample	Annealing temperature, °C	$S_{\text{BET}}$ , m <sup>2</sup> /g
LiCoO <sub>2</sub> -1	700	1.6
LiCoO <sub>2</sub> -2*	700	3.4
LiCoO <sub>2</sub> -3	800	0.7
LiCoO <sub>2</sub> -4*	800	2.4

\*Synthesis included the MA stage.

netic stirrer. Then, the RhCl<sub>3</sub> or H<sub>2</sub>PtCl<sub>6</sub> solution of desired concentration was added, and the resulting suspension was stirred for 15 min at room temperature. Afterwards, the sample was heated to 80 °C and dried under continuous stirring. After impregnation, the catalysts were dried in air at 110–130 °C for 2 h. The metal content was 1 mass %.

To prepare LiCoO<sub>2</sub>, Li<sub>2</sub>CO<sub>3</sub> and Co<sub>3</sub>O<sub>4</sub> were used as reagents. MA was carried out using a planetary mechanical activator APF with steel jars and balls. The time of MA was 3 min. The activated and non-activated mixtures were annealed at 700 and 800 °C for 8 h in air. The main synthesis parameters and the values of surface area for LiCoO<sub>2</sub> samples are presented in Table 1.

The effect of as-prepared LiCoO<sub>2</sub> supports on the activity of Pt and Rh catalysts in the NaBH<sub>4</sub> hydrolysis was compared with traditional supports, such as carbon (Sibunit) [16] with  $S_{\text{BET}} = 530$  m<sup>2</sup>/g and grain size 0.08–0.1 mm;  $\gamma$ -Al<sub>2</sub>O<sub>3</sub> (Katalizator Co.) with  $S_{\text{BET}} = 170$  m<sup>2</sup>/g and grain size smaller than 0.04  $\mu$ m; and TiO<sub>2</sub> (Sigma-Aldrich) with  $S_{\text{BET}} = 243$  m<sup>2</sup>/g.

#### LiCoO<sub>2</sub> and catalyst characterization

The crystal and local structure of as-prepared LiCoO<sub>2</sub> samples was analyzed by XRD and FTIR spectroscopy. Powder diffraction patterns were recorded using DRON-3.0 diffractometer with CuK $\alpha$  irradiation. FTIR spectra were registered in the 200–4000 cm<sup>-1</sup> wavelength range using a Bomem MB-102 Bruker FTIR spectrometer at room temperature. The samples were diluted with CsI and pelletized. Specific surface area of the LiCoO<sub>2</sub> samples was determined using thermal adsorption of argon.

The interaction of LiCoO<sub>2</sub> with NaBH<sub>4</sub> solution was studied by XRD, FTIR and DRS spectroscopy. The DRS spectra were recorded at room temperature in air using a Specord M-40 spectrometer (Carl Zeiss Jena) with a standard diffuse reflectance attachment in the wavelength range 45 000–11 000 cm<sup>-1</sup> and an Interspec 2010 Fourier Transform spectrometer (Spectrolab Co.) with a diffuse reflectance attachment in the wavelength range 10 000–3500 cm<sup>-1</sup>. Particle morphology of LiCoO<sub>2</sub> before and after treatment with NaBH<sub>4</sub> was studied using high resolution transmission electron microscopy (HRTEM). Electron micrographs were obtained with JEM-2010 instrument with lattice resolution 1.4 Å and accelerating voltage 200 kV. Periodic images of lattice structures were analyzed using digital Fourier transformation. Local elemental analysis was performed with EDX method on Energy-Dispersive X-ray Phoenix Spectrometer equipped with Si (Li) detector with energy resolution not worse than 130 eV. Samples were fixed on “holey” carbon films supported on copper grids and investigated with the electron microscope.

#### Hydrogen generation

The hydrogen generation reaction was carried out at 40 °C in a glass temperature-controlled internal mixing reactor equipped with a magnetic stirrer at the 800 rpm stirring rate. The volume of generated hydrogen was measured using a 100-ml gas burette.

Weighted amount of NaBH<sub>4</sub> (0.0465 g; Acros Organics, 98 %) was placed into the reactor and dissolved in 10 ml of distilled water. The catalyst was added in desired metal-to-hydride molar ratio equal to 1 : 2000. Then, the reactor was sealed with an outlet tube connected to volumetric burette.

The hydrogen generation rate ( $W^{50}$ ) was calculated using the following equation:

$$W^{50} = v_{\text{H}_2} t_{1/2}^{-1} m_{\text{Me}}^{-1} \quad (1)$$

where  $W^{50}$  is a reaction rate, ml<sub>H<sub>2</sub></sub>/(g<sub>cat</sub> s);  $v_{\text{H}_2}$  is a volume of hydrogen produced during time  $t_{1/2}$ , ml;  $t_{1/2}$  is a half-reaction time, s;  $m_{\text{Me}}$  is a catalyst mass, g.

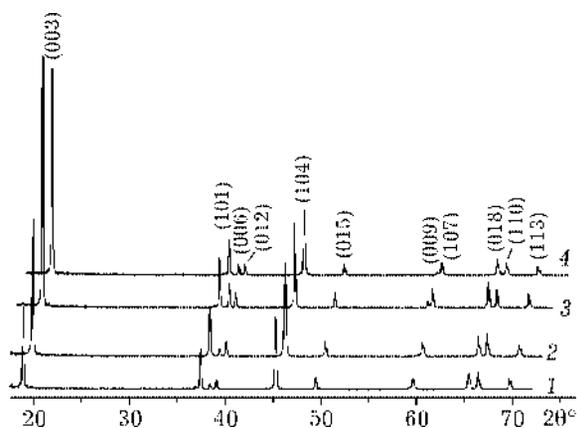


Fig. 1. X-ray diffraction patterns of as-prepared LiCoO<sub>2</sub> samples (see Table 1): 1 - LiCoO<sub>2</sub>-1, 2 - LiCoO<sub>2</sub>-2, 3 - LiCoO<sub>2</sub>-3, 4 - LiCoO<sub>2</sub>-4.

The catalyst endurance tests were carried out at 40 °C. After conversion of the first portion of NaBH<sub>4</sub> (0.0465 g dissolved in 10 ml of distilled water), the catalyst was separated from the reaction mixture and washed with distilled water. Then, the next portion of NaBH<sub>4</sub> was added.

## RESULTS AND DISCUSSION

### LiCoO<sub>2</sub> properties

Depending on the synthetic conditions, it is possible to prepare two different LiCoO<sub>2</sub> modifications: high-temperature (HT) and low-temperature (LT). HT-LiCoO<sub>2</sub> has an ideal layered  $\alpha$ -NaFeO<sub>2</sub> structure (*R3m* space group) with ABCABC oxygen packing. Cobalt and lithium ions are ordered in the octahedral positions of different (111) planes. LT-LiCoO<sub>2</sub> has a spinel-like structure (*Fd3m* space group) where ~6 % of cobalt ions occupy the positions of lithium ions. According to the XRD data (Fig. 1), all as-prepared LiCoO<sub>2</sub> samples corresponded to high-temperature modification HT-LiCoO<sub>2</sub>.

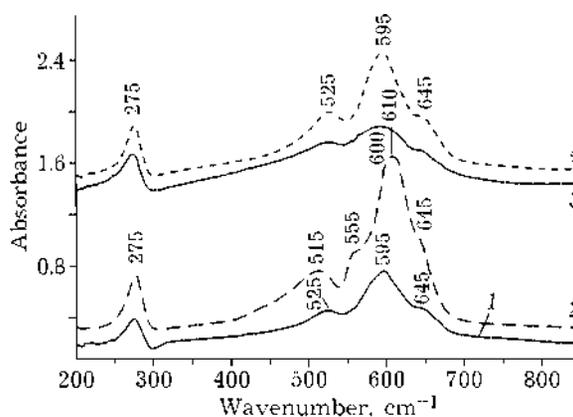


Fig. 2. FTIR spectra of as-prepared LiCoO<sub>2</sub> samples (see Table 1): 1 - LiCoO<sub>2</sub>-1, 2 - LiCoO<sub>2</sub>-2, 3 - LiCoO<sub>2</sub>-3, 4 - LiCoO<sub>2</sub>-4.

The splitting of the 006 and 012; 018 and 010 reflexes was observed in the diffraction patterns, whereas the ratio of the lattice parameters  $c/a$  was equal to 4.99 (Table 2). Both of these features are typical for HT-LiCoO<sub>2</sub>. For LT-LiCoO<sub>2</sub>, these reflexes do not split due to removal of the hexagonal distortion, and  $c/a = 4.90$ . However, the reflexes for samples prepared using MA are wider as compared with ceramic ones. This indicates that the average crystal size of their particles is smaller. This conclusion was confirmed by the surface area data (see Table 1). On the other hand, the intensity ratio of reflexes 003 and 104 was higher for the samples prepared without MA. This ratio grew with the annealing temperature (see Tables 1, 2). To our opinion, this growth reflects an increased textural orientation of the samples. Meanwhile, no significant change of the lattice parameters was observed (see Table 2).

Figure 2 shows FTIR spectra of as-prepared LiCoO<sub>2</sub>. For all the samples, the absorption bands at 640, 600, 555, 515 and 275 cm<sup>-1</sup> are observed. Their positions and intensity ratios are characteristic of HT-LiCoO<sub>2</sub> and close to liter-

TABLE 2

Lattice parameters of synthesized LiCoO<sub>2</sub> samples according to the XRD data

Sample	$a \pm 0.00003$ , nm	$c \pm 0.0002$ , nm	$c/a$	$I_{003}/I_{104}$
LiCoO <sub>2</sub> -1	0.28148	1.4049	4.991	1.43
LiCoO <sub>2</sub> -2	0.28150	1.4055	4.993	1.12
LiCoO <sub>2</sub> -3	0.28151	1.4045	4.989	4.88
LiCoO <sub>2</sub> -4	0.28149	1.4045	4.990	3.13

ature data [17]. The first four bands correspond to vibrations of the  $\text{CoO}_6$  octahedrons, whereas the band at  $276\text{ cm}^{-1}$  is related to vibrations of the  $\text{LiO}_6$  octahedrons. It should be noted that the intensity of the absorption bands of MA samples ( $\text{LiCoO}_2$ -2 and  $\text{LiCoO}_2$ -4 in Table 1) is higher than those of ceramic samples ( $\text{LiCoO}_2$ -1 and  $\text{LiCoO}_2$ -3 in Table 1). To our opinion, this is a result of different amount of delocalized electrons in the systems [18].

### $\text{NaBH}_4$ hydrolysis

The catalyst loaded into the reactor consists of rhodium or platinum chloride supported on lithium cobalt oxide. After its contact with the first portion of  $\text{NaBH}_4$ , the supported rhodium and platinum compounds are quickly reduced to the corresponding metals forming the active component of the catalyst.

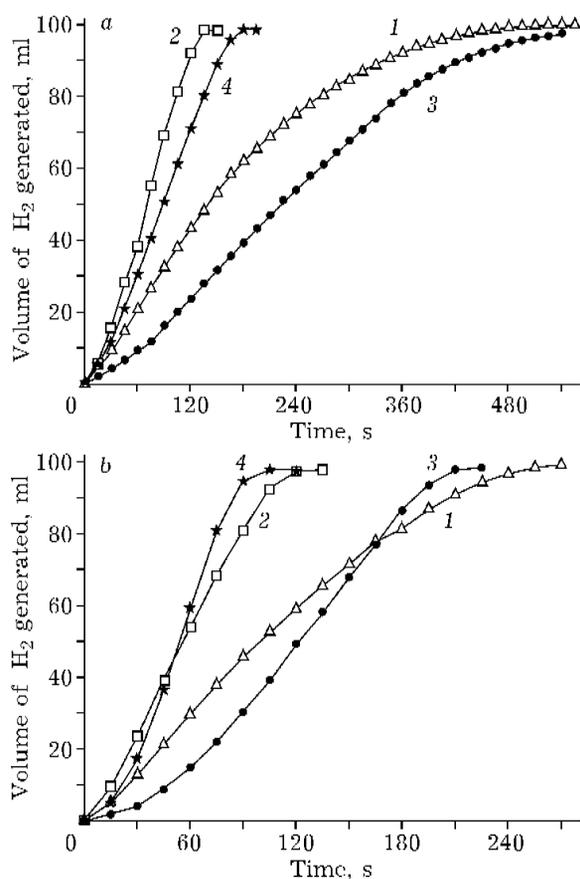


Fig. 3. Cumulative hydrogen generation rate at 40 °C on 1% Rh/LiCoO<sub>2</sub> (a) and 1% Pt/LiCoO<sub>2</sub> (b) catalysts supported on different LiCoO<sub>2</sub> supports (see Table 1): 1 – LiCoO<sub>2</sub>-1, 2 – LiCoO<sub>2</sub>-2, 3 – LiCoO<sub>2</sub>-3, 4 – LiCoO<sub>2</sub>-4.

The investigation of Rh and Pt catalysts supported on as-prepared HT-LiCoO<sub>2</sub> samples in the  $\text{NaBH}_4$  hydrolysis reaction (Fig. 3, a, b) showed that the synthetic conditions significantly influence the activity of the catalysts. The catalysts supported on fine LiCoO<sub>2</sub> samples prepared using the MA stage were the most active. For 1% Rh/LiCoO<sub>2</sub> catalysts, a decrease of the LiCoO<sub>2</sub> annealing temperature from 800 to 700 °C resulted in a significant increase in hydrogen generation rate (see Fig. 3, a). On the other hand, the effect of the LiCoO<sub>2</sub> annealing temperature on the activity of 1% Pt/LiCoO<sub>2</sub> catalysts was different (see Fig. 3, b): for the LiCoO<sub>2</sub> supports prepared at higher temperature, the type of the hydrogen generation curve changes for samples prepared with and without the MA stage and the longer activation stage is observed. Note that the hydrogen generation rate increases with the growth of specific surface area of initial LiCoO<sub>2</sub>.

The activity of catalysts supported on as-prepared LiCoO<sub>2</sub>-2 was compared with others based on traditional supports, such as  $\gamma\text{-Al}_2\text{O}_3$ , TiO<sub>2</sub> (anatase) and carbon (sibunit) (Fig. 4). Despite the lower surface area of LiCoO<sub>2</sub> support as compared with the other supports (see above), the 1% Rh/LiCoO<sub>2</sub>-2 and the 1% Pt/LiCoO<sub>2</sub>-2 catalysts were characterized by significantly higher hydrogen generation rates.

The results of the endurance tests of the 1% Rh/LiCoO<sub>2</sub>-2 and 1% Pt/LiCoO<sub>2</sub>-2 catalysts are presented in Fig. 5, a, b. One can see

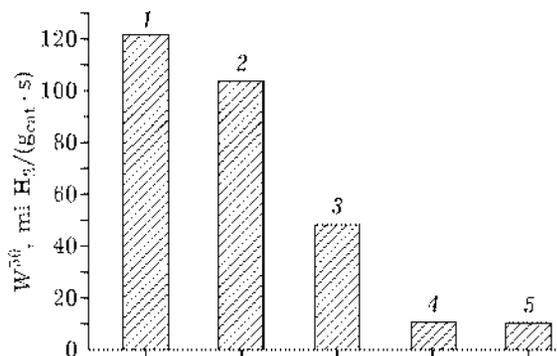


Fig. 4. Cumulative hydrogen generation rate at 40 °C on 1% Pt/LiCoO<sub>2</sub> (a) and 1% Pt/LiCoO<sub>2</sub> catalysts supported on different LiCoO<sub>2</sub> supports (see Table 1): 1 – 1% Rh/LiCoO<sub>2</sub>-2, 2 – 1% Pt/LiCoO<sub>2</sub>-2, 3 – 1% Rh/TiO<sub>2</sub>, 4 – 1% Rh/Sibunit, 5 – 1% Rh/Al<sub>2</sub>O<sub>3</sub>.

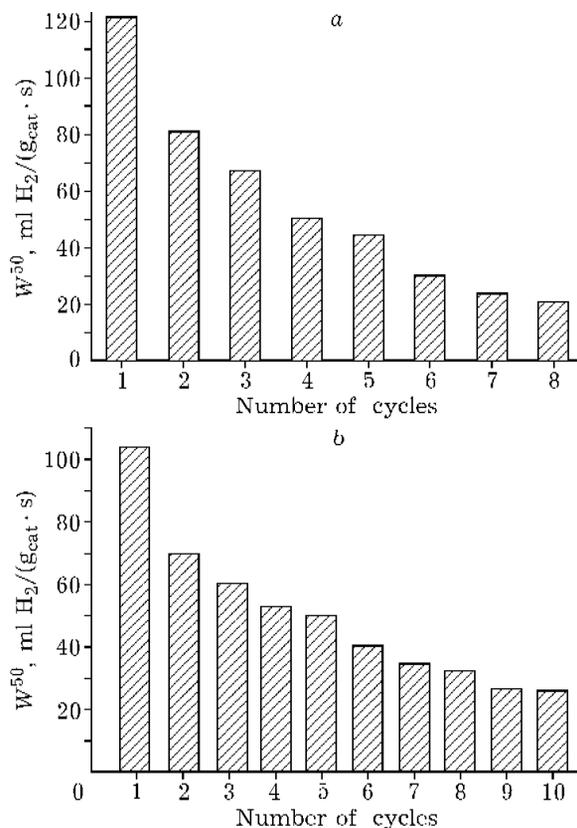


Fig. 5. Endurance tests for H<sub>2</sub> generation rate for 1% Rh/LiCoO<sub>2</sub>-2 (a) and 1% Pt/LiCoO<sub>2</sub>-2 (b) at 40 °C.

that after addition a new NaBH<sub>4</sub> portion, the activity of the catalysts gradually decreases.

Figure 6 presents hydrogen generation rate for the 1% Rh/LiCoO<sub>2</sub>-2 catalyst as a function of time for 1–8 cycles. The 1st cycle is characterized by sharp generation of hydrogen. During the other cycles, hydrogen generation rate dramatically decreased and became much more uniform, however, the total amount of generated hydrogen remains constant. The similar results were obtained for the 1% Pt/LiCoO<sub>2</sub>-2 catalyst.

To understand the reasons of degradation of the LiCoO<sub>2</sub>-supported catalyst activity, we carried out an XRD, FTIR, DRS and TEM investigation of lithium cobalt oxide support after its treatment with NaBH<sub>4</sub> solution.

According to XRD, the intensity of reflexes of LiCoO<sub>2</sub>-2 treated with 1.2 M solution of NaBH<sub>4</sub> at 40 °C is reduced more than twice. However, the lattice parameters remain unchanged. Figure 7 presents the FTIR spectra of LiCoO<sub>2</sub>-2 before (curve 1) and after (curve 2)

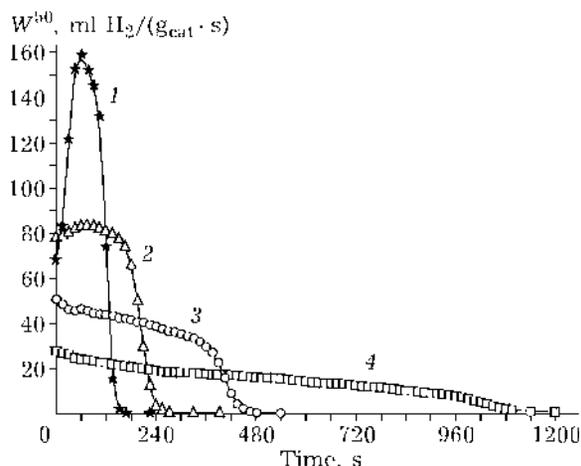


Fig. 6. Hydrogen generation rate for 1% Rh/LiCoO<sub>2</sub>-2 catalyst as a function of time: 1–4 – cycle 1, 2, 5, 8, respectively.

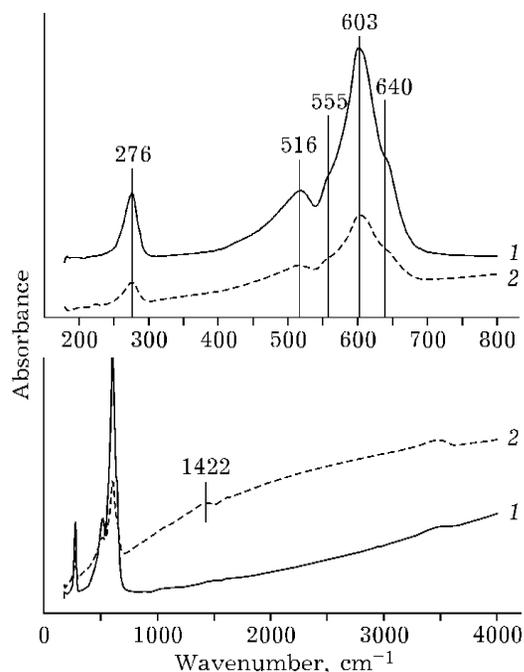


Fig. 7. FTIR spectra of LiCoO<sub>2</sub>-2 (see Table 1) before (1) and after (2) treatment with 1.2 M NaBH<sub>4</sub> solution at 40 °C.

its treatment with NaBH<sub>4</sub>. It shows that the sample treatment does not noticeably affect the positions of the LiCoO<sub>2</sub> absorption bands or their intensity ratios. The low-intensity band at 1422 cm<sup>-1</sup> can be attributed to vibrations of carbonates. Thus, the most part of the LiCoO<sub>2</sub> sample retains its structure. On the other hand, the drop of the intensity of the IR absorption bands and the appearance of significant background absorption are observed.

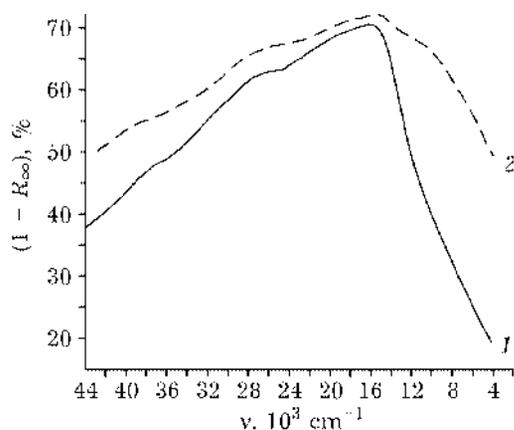


Fig. 8. DRS spectra of LiCoO<sub>2</sub>-2 (see Table 1) before (1) and after (2) treatment with 1.2 M NaBH<sub>4</sub> solution at 40 °C.

Some changes are also observed in the DRS electronic spectrum of treated LiCoO<sub>2</sub>-2 (Fig. 8). Substantial additional absorption, most significant in the near-IR region, appears after reaction (curve 2). Such absorption is typical for metals and metal-like compounds. We suppose that partial LiCoO<sub>2</sub> reduction occurs on the surface

of the particles with the formation of CoB<sub>x</sub> nanoparticles. Cobalt borides of variable composition CoB<sub>x</sub> are known to be formed after Co<sup>2+</sup> reaction with BH<sub>4</sub><sup>-</sup> in aqueous solutions. Their conductivity is close to that of metallic cobalt [19–22].

According to TEM (Fig. 9), the surface of LiCoO<sub>2</sub> particles drastically changes after treatment. The formation of Co particles and glass-like layer, most probably, consisting of lithium boron oxide, are clearly observed. One can suppose that this layer is the reason of catalyst degradation after prolonged cycling because of worsening contacts of metallic catalytic particles with support. However, additional studies are required to prove this hypothesis.

## CONCLUSION

It is shown that the catalysts supported on LiCoO<sub>2</sub> prepared using mechanical activation have the highest catalytic activity in the NaBH<sub>4</sub>

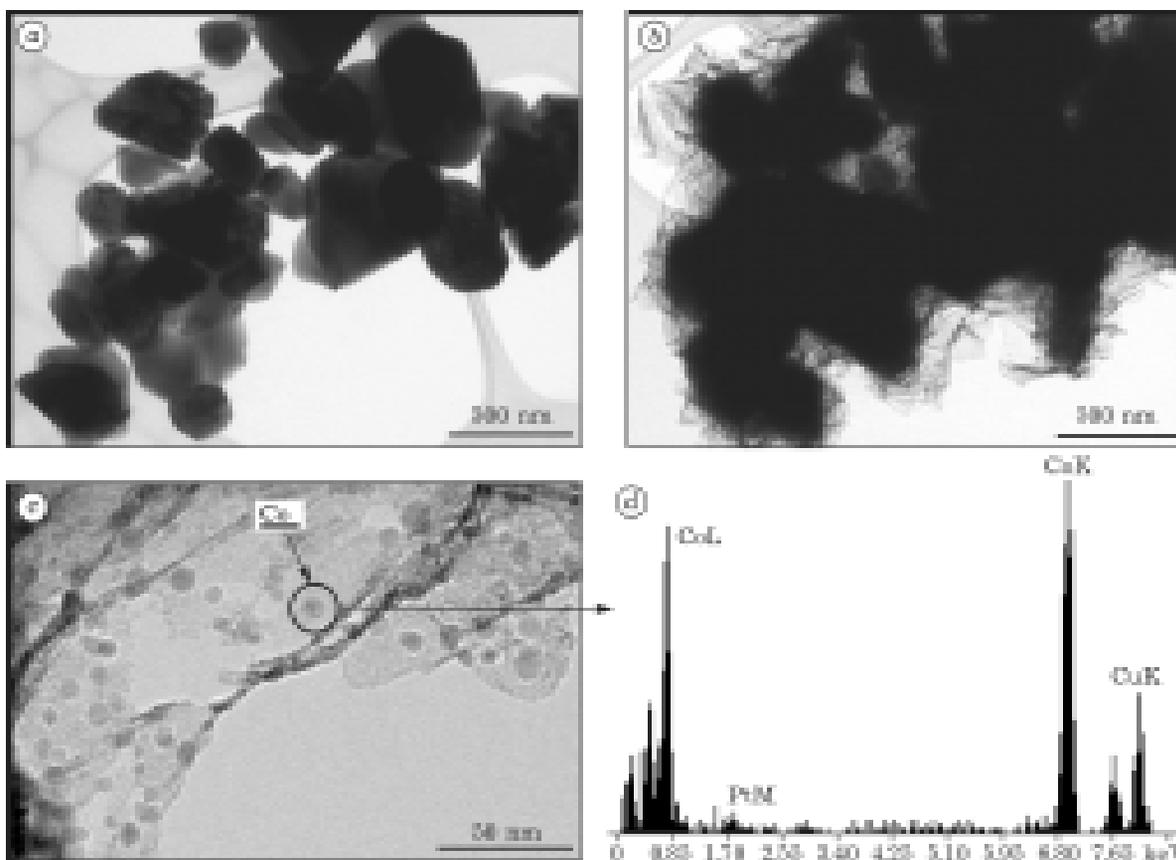


Fig. 9. TEM images of LiCoO<sub>2</sub>-2 (see Table 1) before (a) and after (b, c) treatment with 1.2 M NaBH<sub>4</sub> solution at 40 °C; d – EDX analysis of particle shown in image c.

hydrolysis as compared with catalysts supported on ceramic LiCoO<sub>2</sub> and other traditional supports ( $\gamma$ -Al<sub>2</sub>O<sub>3</sub>, anatase, carbon material). The endurance tests of the catalysts supported on MA-LiCoO<sub>2</sub> showed that their activity gradually decreases with each new portion of converted substrate. This was associated with partial surface interaction of LiCoO<sub>2</sub> particles with a NaBH<sub>4</sub> solution leading to the formation of glass-like lithium boron oxide layer.

### Acknowledgement

We thank Dr. V. I. Zaikovskii for helpful discussion.

### REFERENCES

- 1 H. I. Schlesinger, H. C. Brown, A. E. Finholt *et al.*, *J. Am. Chem. Soc.*, 75 (1953) 215.
- 2 S. C. Amendola, S. L. Sharp-Goldman, M. S. Janjua *et al.*, *J. Power Sources*, 85 (2000) 186.
- 3 Y. Kojima, K. Suzuki, K. Fukumoto *et al.*, *Int. J. Hydrogen Energy*, 27 (2002) 1029.
- 4 B. S. Richardson, J. F. Birdwell, F. G. Pin *et al.*, *J. Power Sources*, 145 (2005) 21.
- 5 S. C. Amendola, S. L. Sharp-Goldman, M. S. Janjua *et al.*, *Int. J. Hydrogen Energy*, 25 (2000) 969.
- 6 Z. T. Xia and S. H. Chan, *J. Power Sources*, in press.
- 7 C. Wu, H. Zhang, B. Yi, *Catal. Today*, 93–95 (2004) 477.
- 8 C. Wu, F. Wu, Y. Bai *et al.*, *Mat. Lett.*, 59 (2005) 1748.
- 9 S. U. Jeong, R. K. Kim, E. A. Cho *et al.*, *J. Power Sources*, 144 (2005) 129.
- 10 D. Hua, Y. Hanxi, Ai. Xinping, C. Chuansin, *Int. J. Hydrogen Energy*, 28 (2003) 1095.
- 11 J.-Ho Kim, Ki-T. Kim, Y.-M. Kang *et al.*, *J. Alloys Comp.*, 379 (2004) 222.
- 12 J.-Ho Kim, Ho Lee, S.-C. Han *et al.*, *Int. J. Hydrogen Energy*, 29 (2004) 263.
- 13 Y. Kojima, Y. Kawai, H. Nakanishi, S. Matsumoto, *J. Power Sources*, 135 (2004) 36.
- 14 Y. Kojima, K.-I. Suzuki, K. Fukumoto *et al.*, *Ibid.*, 125 (2004) 22.
- 15 P. Krishnan, T.-H. Yang, W.-Y. Lee, C.-S. Kim, *Ibid.*, 143 (2005) 17.
- 16 V. F. Surovikin, G. V. Plaxin, V. A. Semikolenov *et al.*, US Pat. 4978649, 1990.
- 17 V. V. Kaichev, N. V. Kosova, E. T. Devyatkina *et al.*, *Rus. J. Phys. Chem.*, 77 (2003) 1445.
- 18 C. Julien, *Solid State Ionics*, 136–137 (2000) 887.
- 19 J. Shen, Z. Li, Q. Yan, Yi Chen, *J. Phys. Chem.*, 97 (1993) 8504.
- 20 C. Petit, M. P. Pileni, *J. Magn. Magn. Mater.*, 166 (1997) 82.
- 21 I. Dragieva, D. Mehandjiev, E. Lefterova *et al.*, *Ibid.*, 140–144 (1995) 455.
- 22 E. Lefterova, I. Dragieva, V. Tchanev *et al.*, *Ibid.*, 140–144 (1995) 457.